Available online at www.sciencedirect.com
SCIENCE DIRECT®
Materials Research Bulletin 39 (2004) 41–54
Materials Research Bulletin
www.elsevier.com/locate/matresbu

# Studies on $LiNi_{0.7}Al_{0.3-x}Co_xO_2$ solid solutions as alternative cathode materials for lithium batteries

P. Kalyani*, N. Kalaiselvi, N.G. Renganathan, M. Raghavan

*Advanced Batteries Division, Central Electrochemical Research Institute, Karaikudi 630 006, India*

Received 18 March 2003; received in revised form 18 August 2003; accepted 5 September 2003

**Abstract**

A series of phase-pure Co- and Al-substituted lithium nickel oxide solid solutions of the composition $LiNi_{0.7}Al_{0.3-x}Co_xO_2$ with $x = 0.0$, 0.1, 0.15, 0.2, and 0.3, has been synthesized by adopting urea-assisted combustion (UAC) route. The structure and the physico-electrochemical features of the doped materials have been evaluated through PXRD, FTIR, SEM, CV, and charge/discharge studies. The stabilization of Ni in the +3 state and the existence of enhanced 2D-layered structure without any cation mixing have been substantiated from XRD. The results of the XRD and FTIR studies have established the complete mixing of Al and Co with Ni, especially at the various levels and the combinations of the dopants attempted in the present study. The enhanced electrochemical performance of $LiNi_{0.7}Al_{0.3-x}Co_xO_2$ may be attributed to the ''synergetic effect'' resulting from the presence of both $Al^{3+}$ and $Co^{3+}$ dopants in the $LiNiO_2$ matrix. From CV studies, it was understood that the addition of 10% Co is effective in suppressing the phase transformation during $Li^+$ intercalation process that leads to better electrochemical properties. The effect and the extent of substitution of Ni with Al and Co on the structural and electrochemical performance of $LiNi_{0.7}Al_{0.3-x}Co_xO_2$ are discussed elaborately in this communication.


*Keywords:* A. Layered compounds; A. Oxides; B. Intercalation reactions; C. X-ray diffraction; D. Electrochemical properties

## 1. Introduction

Lithiated transition metal oxides like $LiMn_2O_4$ [1] and $LiCoO_2$ [2] are currently being utilized as the principal cathode materials for fabricating lithium batteries, since they possess high voltage, high capacity, and energy density. A thorough knowledge about these two compounds has been acquired, in terms of their synthesis methods, to achieve maximum electrochemical activity. To demonstrate this,

* Corresponding author. Tel.: +91-4565-227-555; fax: +91-4565-427-779.
*E-mail address:* kalyani_1973@yahoo.com (P. Kalyani).

0025-5408/$ – see front matter © 2003 Elsevier Ltd. All rights reserved.
doi:10.1016/j.materresbull.2003.09.021

over a decade, Bellcore and Sony Energytec Inc. are commercializing lithium cells with $LiMn_2O_4$ and $LiCoO_2$ cathodes, respectively [3]. But, the frequently reviewed analog of $LiCoO_2$ namely, $LiNiO_2$, though has been bestowed with a higher capacity of about 190 mAh/g [4] (compared to $LiMn_2O_4$ and $LiCoO_2$), poses complications in terms of the synthesis conditions. That is, thermal and electrochemical instability, phase transitions upon cycling [5], and safety problems due to the exothermic decomposition [6] (by liberating oxygen, when $LiNiO_2$ is inadvertently overcharged) are the common problems associated with the layered nickel oxide cathodes synthesized under ambient conditions. To circumvent these problems, stringent synthesis conditions are highly essential to obtain the compound in its pure, stoichiometric, and consistent form [7,8]. This in turn leads to the possibility of possessing perfect 2D-layered characteristics without cation mixing and an enhanced cell capacity of $LiNiO_2$ cathodes by the removal of $Ni^{2+}$ ions occupying the $Li^+$ sites that retard the diffusion of $Li^+$. In this context, various metal cation-substituted/modified $LiNiO_2$ cathode materials viz., the solid solutions of $LiNi_{1-x}M_xO_2$ [9–11] category (M = Mg, Mn, Co, etc., or combination of these dopants) have been identified with a view to find their application in lithium batteries with improved electrochemical properties. Such materials require less severe synthesis conditions, possess high reversible capacity and are also electrochemically stable, i.e. do not undergo phase transformations during the charge/discharge processes.

Of these various cathodes, substituted compounds of the general formula $LiNi_{1-x}Co_xO_2$ [12] have been identified as one the most attractive materials as they exhibit synergetic effect in terms of enhanced stabilization of 2D structure, extended cyclability, improved capacity, etc., that originate from the combined effects of the highly cyclable $LiCoO_2$ and the high capacity $LiNiO_2$. Among the dopants studied, aluminum has been of profound interest with respect to both $LiNiO_2$ [13–15] and $LiCoO_2$ [14] cathodes, due to its low atomic mass and cost. Based on the suggestions of Alcántara et al. [16] and the recommendations of Ohzuku et al. [13], it is believed that the $Al^{3+}$ substitution favors the stabilization of Ni in the +3 oxidation state and enhances the existence of two dimensionality of the layered structure, which leads to the suppression of phase transition during electrochemical cycling ultimately. Since Al cannot be oxidized or reduced beyond +3 state, the maximum amount of intercalated or deintercalated lithium can also be limited, depending upon the Al content. Hence partial substitution of Al for Ni prevents the cell from over charging, and hence is responsible for cell safety [13,17]. Further, advantages of partial substitution of Al in to the crystal structure of $LiCoO_2$ has been reported by Ceder and coworkers [18,19] in their ab initio studies, that an increase in cell voltage could be achieved by Al substitution by forcing more electronic exchange between lithium and the oxygen network.

In the present study, a newer class of materials of the formula $LiNi_{0.7}Al_{0.3-x}Co_xO_2$ has been synthesized and analyzed for their suitability as cathode materials for lithium batteries. The preference for the 70% of Ni in these compounds originated from a similar observation made by Subba Rao and coworkers [20] in $LiNi_{0.7}Co_{0.3-z}Al_zO_2$, wherein the usage of 70% of Ni has been established to achieve enhanced charge retention and cycling efficiency. In recent years, the solution combustion technique, which involves the usage of urea together with the corresponding metal nitrates (the urea-assisted combustion(UAC) method), has attracted the attention of researchers, as it leads to the production of homogeneous, fine and un-agglomerated multi-component oxide powders without involving intermediate decomposition and/or calcinations steps [21]. Also, solution preparative techniques allow atomic level mixing of the elements and thus phase-pure products can easily be achieved. The significance and flexibility of the UAC method has already been established by way of synthesizing a

variety of other lithium battery cathodes like $LiCoO_2$ [22], $LiMn_2O_4$ [23], $LiNi_{1-x}Co_xO_2$ [24], $LiNi_{0.7}Al_xB_yO_2$ [25], etc., by various research groups and also by the authors of this communication. More specifically, this paper highlights the unique attempt of evaluating the electrochemical performance of the title compounds synthesized by the solution combustion method namely, the UAC method.

## 2. Experimental aspects

### 2.1. Sample preparation

The substituted nickel oxides of the general formula $LiNi_{0.7}Al_{0.3-x}Co_xO_2$ ($x = 0.0, 0.1, 0.15, 0.2$, and 0.3) have been synthesized by the solution combustion route [26,27] using urea as the fuel to aid the combustion process (Fig. 1). Calculated amounts of urea and nitrates of lithium, nickel, aluminum, and cobalt were dissolved in hot distilled water to get a homogenous solution. The amount of urea was calculated based on the procedure given in Ref. [26] and the mixture was heated slowly to

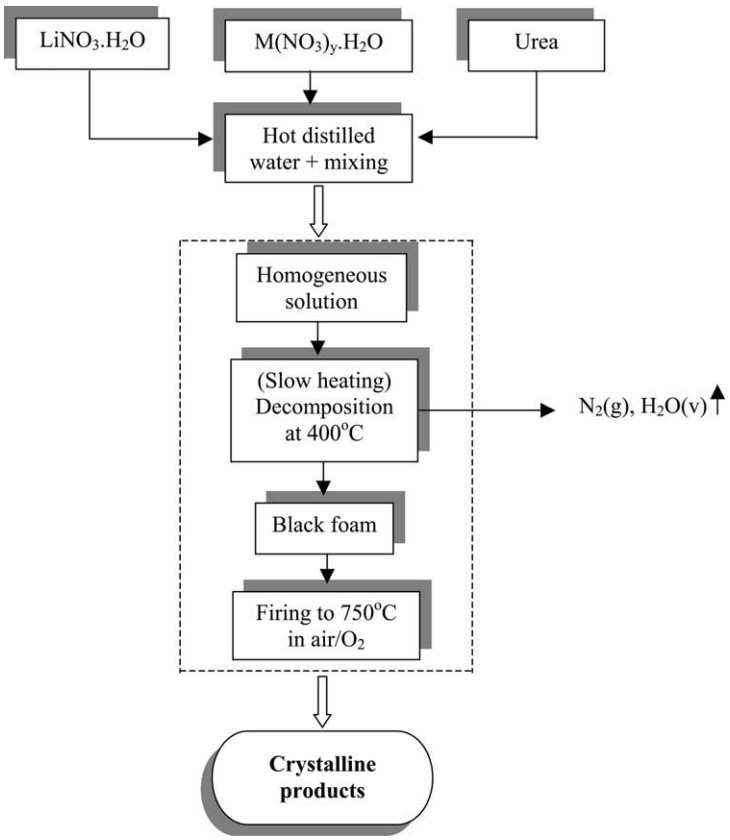


Fig. 1. Schematic representation of the synthesis of $LiNi_{0.7}Al_{0.3-x}Co_xO_2$ compounds by UAC route (M = Ni, Al, and Co).

Table 1
Optimized synthesis conditions and refined unit cell crystal parameters of $LiNi_{0.7}Al_{0.3-x}Co_xO_2$

| Compound | Lattice constants | | | | | | | | |
|---|---|---|---|---|---|---|---|---|---|
| | Temperature (°C) | DT (h) | $a$ (Å) | $c$ (Å) | Unit cell volume (Å$^3$) | $c/a$ | $I_{(0\,0\,3)}/I_{(1\,0\,4)}$ | Density (g/cm$^3$) | Surface area (m$^2$/g) |
| $LiNi_{0.7}Al_{0.3}O_2$ | 750 | 32 | 2.849 | 14.152[a] | 99.512 | 4.967 | 1.11 | 4.194 | 15 |
| $LiNi_{0.7}Al_{0.2}Co_{0.1}O_2$ | 750 | 10 | 2.861 | 14.196[b] | 100.630 | 4.962 | 1.18 | 4.026 | 15 |
| $LiNi_{0.7}Al_{0.15}Co_{0.15}O_2$ | 750 | 10 | 2.859 | 14.198[b] | 100.502 | 4.966 | 1.21 | 3.687 | 17 |
| $LiNi_{0.7}Al_{0.1}Co_{0.2}O_2$ | 750 | 10 | 2.862 | 14.162[b] | 100.457 | 4.948 | 1.28 | 3.987 | 18 |
| $LiNi_{0.7}Co_{0.3}O_2$ | 750 | 10[c] | 2.857 | 14.075[d] | 99.500 | 4.926 | 1.28 | 4.161 | 18 |

DT, dwelling time.
[a]Ref. [13].
[b]Ref. [20].
[c]In flowing $O_2$ atmosphere.
[d]Ref. [12] for comparison of $a$ and $c$ data.

400 °C for about 30 min. The process of slow heating ensures slow and uniform combustion of the mixture and the same has resulted in the formation of black foam. The foam thus obtained was then crushed and the powdered sample was further subjected to a firing sequence in air or flowing $O_2$ atmosphere at a temperature of 750 °C for about 10–32 h, depending upon the requirement, which is given in Table 1.

### 2.2. Instrumental

Phase characterization was done by powder X-ray diffraction technique using JEOL-JDX 8030 X-ray diffractometer using Ni filtered Cu Kα radiation ($\lambda = 1.5406$ Å) in the $2\theta$ range of 10–80° at a scan rate of 0.1°/s. FTIR spectra were recorded with Perkin-Elmer Paragon-500 FTIR Spectrophotometer using KBr pellets in the region 400–1000 cm$^{-1}$. Density of the powders was determined by the method based on Archimedes' principle of liquid displacement [28], using xylene medium. Surface morphology of the particles was examined from the Scanning Electron Micrographs obtained from Hitachi S-3000 H Scanning Electron Microscope and the particle size of the oxide materials was determined using Malvern Easy Particle sizer. Surface area of the synthesized powders was determined by BET adsorption method using low temperature nitrogen adsorption (Quanta Chrome Nova 1000, US).

Electrochemical performance was evaluated by assembling cathode-limited 2016 lithium coin cells. Cathodes were fabricated by slurrying the cathode powders with 10% graphite and 2% PVdF as binder in *N*-methyl-2-pyrrolidone (NMP) as solvent and coating the mixture over Al foil (serves as current collector). After drying at 110 °C overnight, the discs were pressed in a hydraulic press by applying a pressure of about 10–15 kg/cm$^2$ for perfect adherence of the coated material over the surface of the Al current collector. Discs of 1.6 cm diameter were punched out and typical cathodes were found to have an average active material coverage of about 10–15 mg per disc. Electrolyte consisted of 1 M $LiAsF_6$ dissolved in equal volumes of EC and DMC and the separator used was polypropylene fabric. Charge/discharge studies were performed using an in-house cell-testing unit. Cyclic voltammograms were recorded using ''AUTOLAB'' software controlled by a Personal Computer.

## 3. Results and discussion

### 3.1. Effect of substituents versus synthesis conditions

The effect of incorporating cobalt in $LiNi_{0.7}Al_{0.3}O_2$ compounds towards the reduction of the duration of heat treatment is obvious from Table 1. For better clarity and understanding, the synthesized compounds may be viewed as Co-substituted lithium aluminum nickelates ($LiNi_{0.7}Al_{0.3-x}Co_xO_2$; $x = 0.1$, 0.15, and 0.2) and the end member solid solutions viz., $LiNi_{0.7}Al_{0.3}O_2$ ($x = 0.0$) and $LiNi_{0.7}Co_{0.3}O_2$ ($x = 0.3$), wherein Al or Co substitutes partially for Ni in $LiNiO_2$ matrix.

In the series of five compounds, the synthesis of $LiNi_{0.7}Al_{0.3}O_2$ (containing Al as the only dopant) required a temperature of at least 750 °C and a dwelling time of about 32 h. This suggests that the incorporation of Al as a dopant in $LiNiO_2$ may preclude the necessity of $O_2$ atmosphere in producing phase-pure oxides, despite the fact that its immediate parent compound namely, $LiNiO_2$ is synthesized exclusively in $O_2$ atmosphere at 750 °C for about 21 h (e.g. Ref. [25]). Therefore, such a compound of interest viz., $LiNi_{0.7}Al_{0.3}O_2$ has been chosen as the parent compound of the present study. Moreover, with a view to minimize the other parameter namely, the period of heat treatment required for the synthesis and also to have tailor-made cathodes for practical applications, introduction of some other dopant in $LiNi_{0.7}Al_{0.3}O_2$ was thought of. In this regard, Co has been identified as the dopant and was found to lessen the duration of heat treatment of $LiNi_{0.7}Al_{0.3}O_2$ significantly from 32 to 10 h, i.e. the incorporation of Co in $LiNi_{0.7}Al_{0.3}O_2$ (to yield $LiNi_{0.7}Al_{0.3-x}Co_xO_2$ solid solutions) not only excluded the heat treatment in $O_2$ atmosphere but also minimized the period of heat treatment. However, the Co substitution in $LiNiO_2$ has been carried out in $O_2$ atmosphere, in view of obtaining phase-pure $LiNi_{0.7}Co_{0.3}O_2$ and hence better electrochemical properties. This observation implies that Al and Co as dopants are effective in making the synthesis conditions less severe. This may also be viewed as the "synergetic effect" of Al and Co dopants, which seems to hold the key in improving the electrochemical performance of the compounds, which will be discussed elaborately in the electrochemical characterization section. Out of the several trials attempted, the heat-treating conditions which has yielded phase-pure and crystalline oxides has been taken as the optimized conditions for synthesizing Al- and/or Co-substituted $LiNiO_2$ viz., $LiNi_{0.7}Al_{0.3-x}Co_xO_2$ and the same has been furnished in Table 1.

### 3.2. Phase analysis by PXRD

Fig. 2 (with insets a and b) represents the PXRD profiles of the $LiNi_{0.7}Al_{0.3-x}Co_xO_2$ samples with $x = 0.1$, 0.15, and 0.2 and the end members (viz., $LiNi_{0.7}Al_{0.3}O_2$ and $LiNi_{0.7}Co_{0.3}O_2$), respectively, processed under the conditions mentioned in Table 1. All the XRD patterns of $LiNi_{0.7}Al_{0.3-x}Co_xO_2$ powders show the formation of single-phase products with a well-defined layered structure without any impure phases observed in the range of substitution of $x = 0.0$–0.3, attempted in the present investigation. The Bragg peaks were indexed assuming a rhombohedral structure (space group: $R\text{-}3m$—$D^5_{3d}$), that are comparable with the earlier reports [12,13,20]. The clear splitting of the hexagonal (1 0 8) and (1 1 0) doublet peaks observed invariably for all the doped derivatives are quite obvious from Fig. 1, which indicates that the compounds possess typical layered characteristics [29]. The crystal constants "$a$" and "$c$" and unit cell volume (determined by an iterative least squares refinement method using the indexed "$h$, $k$, $l$" values), $I_{(0\,0\,3)}/I_{(1\,0\,4)}$, and $c/a$ values of the synthesized solid solutions are given in Table 1.

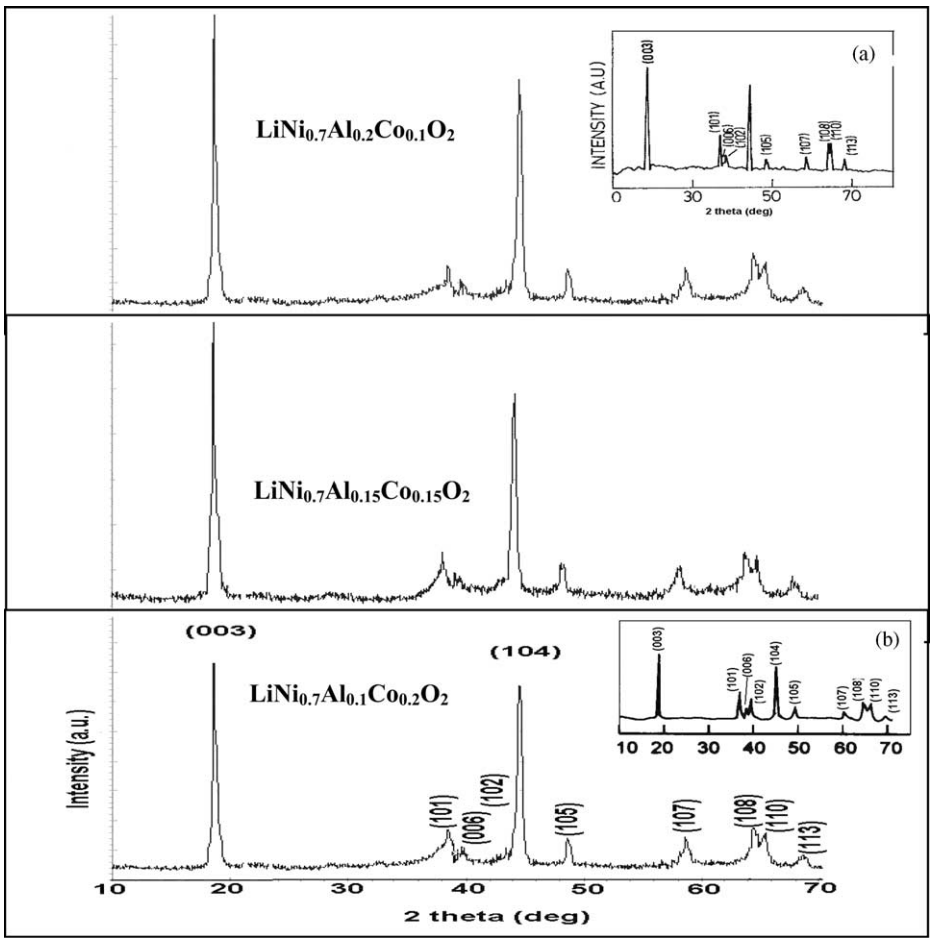


Fig. 2. PXRD patterns observed for the $LiNi_{0.7}Al_{0.3-x}Co_xO_2$ compounds. Inset: (a) $LiNi_{0.7}Al_{0.3}O_2$ and (b) $LiNi_{0.7}Co_{0.3}O_2$.

The degree of trigonal distortion, which is normally expressed as "*c*/*a*" ratio, was found to be greater than 4.9 for all the synthesized compounds, an indication of the high cation ordering [30]. Furthermore, the $I_{(0\,0\,3)}/I_{(1\,0\,4)}$ ratio has a direct impact on the electrochemical properties of the system. It has been used as an indicator for cation mixing in the case of doped layered systems [9]. Values lower than 1.1 indicates a high degree of cation mixing, primarily due to the occupancy of dopant ions in the lithium interslab region. In the present case, the $I_{(0\,0\,3)}/I_{(1\,0\,4)}$ value of various compounds were found to be around 1.20, a value which shows the absence of cation mixing and hence better battery activity of the compounds is highly probable. Interestingly, the unit cell volume of both the Al alone ($LiNi_{0.7}Al_{0.3}O_2$) and Co alone ($LiNi_{0.7}Co_{0.3}O_2$) substituted nickel oxides is observed to be almost the same and is smaller than the Co-substituted $LiNi_{0.7}Al_{0.3}O_2$ samples. The observed increase in the cell volume of the substituted oxides may be attributed to the preferential expansion of the oxide lattice in the "*c*" direction, as a consequence of the substitution of Al and Co for Ni in the original $LiNiO_2$ lattice. Also among the samples substituted with Al and Co, shrinkage

in unit cell volume has been observed with the increasing addition of Co, a factor that has a direct relevance and a remarkable significance with respect to the structural stability and maintenance of capacity upon cycling.

It is well known from many reports [31,32] that, $Ni^{3+}$and $Co^{3+}$ occupies the crystallographically equivalent 3*a* sites and $Li^{+}$ to occupy the 3*b* sites (in $LiNi_{1-x}Co_xO_2$ series) of the rhombohedral structure. Nevertheless, the occupancy of Al is debatable still [16]. Also, it is reported that, aluminum ions do not perturb the layered structure of the compound [16,19,33], and therefore the effect and occupancy of Al cannot be explained completely by XRD. However, based on the reported results of $^{27}Al$ MAS NMR [16], a possible occupancy of a larger amount of aluminum ions in the regular octahedral 3*a* sites and a smaller amount of Al in the tetrahedral 6*c* sites are expected to occur in the present case also. It is further substantiated from the forthcoming characterization studies such as FTIR and CV that the possible occupancy of interstitial 6*c* sites by a lesser fraction of Al cannot be neglected. Similarly, it is worth mentioning here that the interstitial tetrahedral site occupancy of Al, if any, could lead to hindered lithium ion diffusion in the aluminum containing solid solutions [16]. Consequently, the presence of a smaller fraction of interstitial Al may have a negative impact in the electrochemical behavior of the cathodes. Though the observed PXRD data and the subsequent charge/discharge results are in favor of the interstitial 6*c* site occupancy of lesser fraction of Al with the larger proportion in the regular octahedral 3*a* sites, the presence of Al in the interstitial sites can be confirmed only with neutron diffraction or through any structural refinement program.

### 3.3. Local structure by FTIR analysis

The FTIR spectroscopic data show the local structure of the oxide lattice constituted by $LiO_6$ and $MO_6$ octahedra. It is well known that the relative IR absorbance is sensitive to the short-range environment of oxygen coordination around the cations in the oxide lattices, crystal geometry and the oxidation states of the cations involved and is less likely to get affected by the grain size and the morphology or long-range order of the crystal lattice. In other words, it is generally not possible to assign specific IR frequencies to vibrations involving a single cation and its oxide neighbors [34], because the resultant vibrations of any transition metal oxide may involve contributions from all possible atoms. Therefore, it is only the differences in mass, charge, and covalency of lithium and the transition metal cation that leads to the motion of lithium ion and the observation of respective vibrational spectrum [35]. Also, it is customary that the middle frequency region of FTIR (400–700 $cm^{-1}$) is mainly considered for the analysis and hence the present study is restricted to the assignment of various vibrational modes of transition metal oxide cathodes within the frequency range of 400–1000 $cm^{-1}$. As the resonance frequencies of the alkali metal cations in the octahedral interstices ($LiO_6$) in inorganic oxides were reported to be located in the frequency range of 200–400 $cm^{-1}$ [36,37], an elaborate discussion regarding the presence of $LiO_6$ octahedra becomes impossible in the present study for the reasons of instrumental constraints.

The FTIR spectrum of the substituted nickelate compounds is shown in Fig. 3a–e, wherein three FTIR bands appeared prominent invariably for all the oxides. FTIR signature observed near 860 $cm^{-1}$ indicates the presence of Ni–O bond. Similarly, a shift towards lower wavelength, in both the stretching as well as the bending vibrational bands with contraction in unit cell volume upon cobalt substitution has been observed, which in turn confirmed the formation of mixed lithium–nickel–aluminum–cobalt

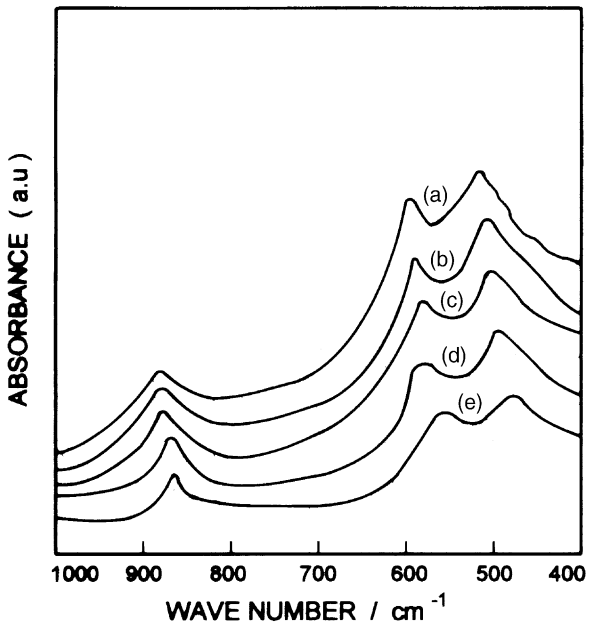


Fig. 3. FTIR spectra of (a) $LiNi_{0.7}Al_{0.3}O_2$, (b) $LiNi_{0.7}Al_{0.2}Co_{0.1}O_2$, (c) $LiNi_{0.7}Al_{0.15}Co_{0.15}O_2$, (d) $LiNi_{0.7}Al_{0.1}Co_{0.2}O_2$, (e) $LiNi_{0.7}Co_{0.3}O_2$.

oxide solid solution. The band observed in the range of 590–551 $cm^{-1}$ may be ascribed to the asymmetric stretching of M–O bonds in $MO_6$ octahedrons and the other one around 515–490 $cm^{-1}$ to the bending modes of O–M–O bonds [24]. These spectroscopic observations establish that the layered structure is well preserved even at the atomic level also. Individual peak assignments for $LiNi_{0.7}Al_{0.3-x}Co_xO_2$ compounds are furnished in Table 2.

### 3.4. Other physical and chemical properties

BET surface area was measured to be around 15–18 $m^2/g$ for the oxide samples. The powder density of the compounds was measured to be about 85–95% of the theoretical density values calculated from the crystal constants and have been included in Table 1. The density value of Co-substituted oxides is

Table 2
FTIR signatures observed for $LiNi_{0.7}Al_{0.3-x}Co_xO_2$ compounds

| Material | Peak assignment ($cm^{-1}$) | |
|---|---|---|
| | $\nu_{M-O}$ stretching | $\delta_{O-M-O}$ bending |
| $LiNi_{0.7}Al_{0.3}O_2$ | 590 | 515 |
| $LiNi_{0.7}Al_{0.2}Co_{0.1}O_2$ | 583 | 508 |
| $LiNi_{0.7}Al_{0.15}Co_{0.15}O_2$ | 575 | 500 |
| $LiNi_{0.7}Al_{0.1}Co_{0.2}O_2$ | 567 | 490 |
| $LiNi_{0.7}Co_{0.3}$ | 551 | 490 |

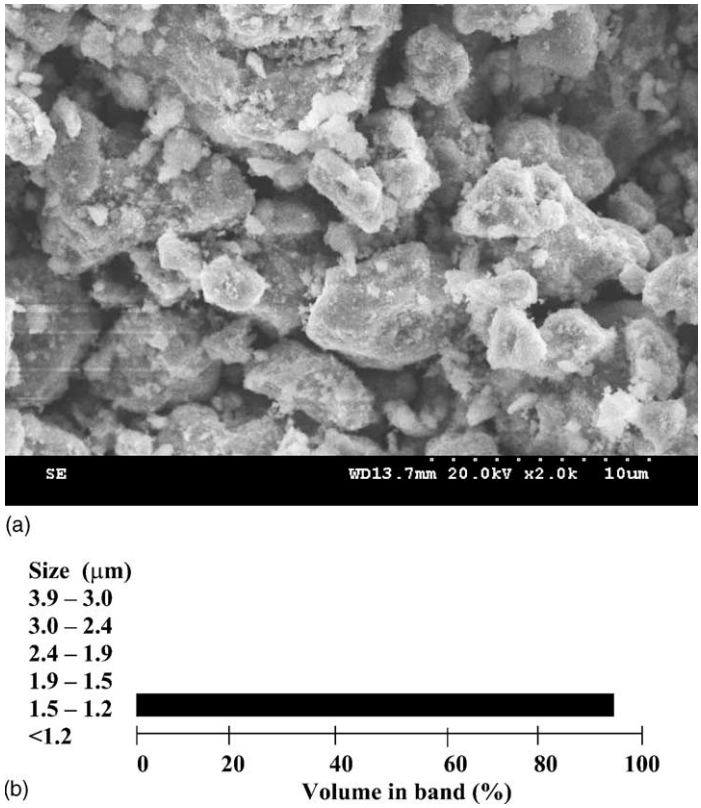


Fig. 4. (a) SEM of $LiNi_{0.7}Al_{0.15}Co_{0.15}O_2$. (b) Particle size distribution in $LiNi_{0.7}Al_{0.15}Co_{0.15}O_2$.

found to be slightly higher than the ''aluminum-alone'' containing nickel oxide sample. This increase in density values is due to the heavier atomic mass of Co compared to the lighter Al dopant. Evidently, the observed density values are in support of the fact that the products obtained from the urea nitrate combustion method are well condensed and sintered.

SEM analysis reveals the nature, shape, approximate grain size, and surface morphology of the particles. All the compositions were found to have an identical morphology and texture, with clearly seen grain boundary. Typical SEM image captured under a magnification of 2K× for $LiNi_{0.7}Al_{0.15}Co_{0.15}O_2$ sample is depicted in Fig. 4, which confirms the presence of growth controlled particles of sub-micron size, a desirable factor [38,39] for exhibiting better electrochemical properties. It is worth to mention here that SEM analysis has been carried out mainly to discuss the morphology of the synthesized compound. SEM, which is the magnification of the selected portion of the sample, represents the averaged out size of the particles. However, particle size and distribution analysis must correspond to the actual size of the particles and the comparison of the same with the values derived from SEM picture need not be considered with due importance. Accordingly, a single and a narrow band (Fig. 4b) observed in the particle size range (1.2–1.6 μm) is an evidence for the uniform distribution of the reduced sized particles. Few percent of the particles are likely to fall even below 1.2 μm.

## 4. Electrochemical characterization

### 4.1. Cyclic voltammetry

Fig. 5 shows the cyclic voltammogram of Li//$LiNi_{0.7}Al_{0.3-x}Co_xO_2$ ($x = 0.10$, 0.15, and 0.3) cells fabricated as 2016 coin type, using a mixture of 1 M $LiAsF_6$ in EC and DMC (1:1, v/v) as the electrolyte. The CV recorded between 3.6 and 4.4 V at a scan rate of 0.1 mV/s indicates that with the increasing cobalt content, the $Li^+$ intercalation voltage is slightly increased i.e. for the compositions with $x = 0.0$, 0.15, and 0.3, the $Li^+$ intercalation voltage has been evaluated to be around 3.79, 3.95, and 4.10 V, respectively.

The evolution of two peaks in the $LiNi_{0.7}Al_{0.3}O_2$ partially suggests that this compound is susceptible to phase transition during the cathodic process of $Li^+$ intercalation, though the origin of the second shoulder around 4.1 V is not clear. On the other hand, no such phase transition was observed for the remaining two compositions studied. This may possibly be viewed as due to the addition of Co that has played a vital role upon the suppression of phase transition [40] and that of insufficient amount of Al (15%) that has failed to induce phase transition in the parent $LiNiO_2$ matrix. However, at this point, it cannot be concluded whether the very presence of Al itself can cause phase transition (the second shoulder at 4.1 V) or an optimum level of Al content could be admissible in to the $LiNiO_2$ matrix, which can preserve the layered structure without inducing any such phase transition. Hence, the observed CV pattern for the various amount of Al taken up for the present study has stimulated an interest to understand the effective role of Al dopant in $LiNiO_2$ especially towards phase transition characteristics. Consequently, optimization of Al dopants (starting from a minimum level of 1%)

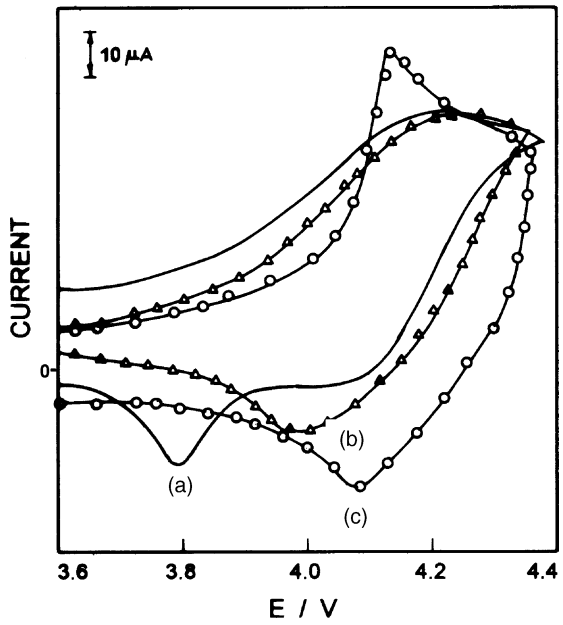


Fig. 5. CV of Li//$LiNi_{0.7}Al_{0.3-x}Co_xO_2$ cells: (a) $LiNi_{0.7}Al_{0.3}O_2$ ($x = 0$); (b) $LiNi_{0.7}Al_{0.15}Co_{0.15}O_2$ ($x = 0.15$); (c) $LiNi_{0.7}Co_{0.3}O_2$ ($x = 0.3$) (scan rate = 0.1 mV/s).

responsible for the consistency of $LiNiO_2$ matrix has been taken up as a separate study. Furthermore, the presence of Co alone or Co in combination with 10% of Al may prove useful in suppressing phase transitions, leading to acceptable electrochemical characteristics. Also, it is interesting to note that there is a significant shift in the cathodic peak towards higher voltages upon increasing cobalt substitution in these substituted nickel oxide samples. As a result, the voltage difference between anodic and cathodic peaks has been narrowed down which is an indication of the high $Li^+$ reversibility.

On the contrary, the large difference between the anodic and cathodic peaks observed for $LiNi_{0.7}Al_{0.3}O_2$ may be attributed to the partial occupancy of Al in the interstitial 6*c* sites of nickel oxide crystal structure. One possible reason for this observation may be due to the increase in cell polarization, as a consequence of slow $Li^+$ diffusion. Therefore, as already mentioned in the XRD analysis, the hindered $Li^+$ diffusion due to the interstitial occupancy of Al has further been substantiated from the CV studies also.

### 4.2. Charge/discharge studies

Charge/discharge cycling has been performed at a current density of 0.1 mA/cm$^2$ between the cut-off voltages of 3 and 4.5 V. Fig. 6 shows the cyclability of the Li//$LiNi_{0.7}Al_{0.3-x}Co_xO_2$ cells up to 15 cycles. It is interesting to note that the first cycle irreversible capacity loss associated with these materials is almost negligible and capacity loss was observed only after the third cycle. The trend observed in the capacity and its fade is as follows. A maximum capacity of about 145 mAh/g has been realized for $LiNi_{0.7}Al_{0.3}O_2$, which showed a significant capacity fade of about 10% at the end of 15 cycles. This result coincides with that of the observation of Ohzuku et al. [17]. The very same trend was observed for the compounds containing 15 and 20% of Al viz., $LiNi_{0.7}Al_{0.15}Co_{0.15}O_2$ and $LiNi_{0.7}Al_{0.2}Co_{0.1}O_2$. On the other hand, the compound $LiNi_{0.7}Al_{0.1}Co_{0.2}O_2$ containing 10% Al has

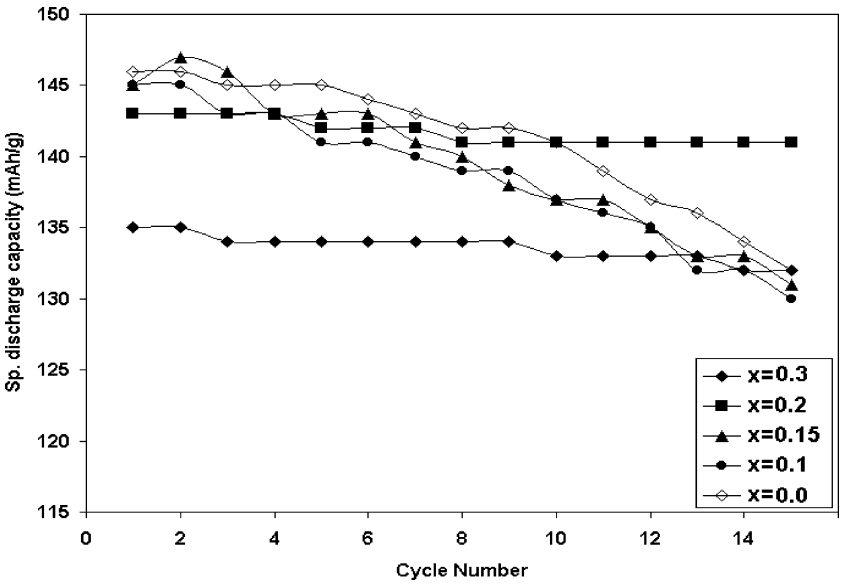


Fig. 6. Cyclability of Li//$LiNi_{0.7}Al_{0.3-x}Co_xO_2$ cells ($cd$ = 0.1 mA/cm$^2$).

delivered about 145 mAh/g without any significant capacity fade. More specifically, the fade was estimated to be only 2%, demonstrating excellent battery activity and cyclability throughout the 15 cycles. Further, it is interesting to note that the compound without Al, i.e. $LiNi_{0.7}Co_{0.3}O_2$, exhibited an excellent cell cyclability delivering a capacity of about 135 mAh/g throughout. Though the initial discharge capacity of this compound was found to be lesser than the rest of the compounds in the series, the cycling performance of $LiNi_{0.7}Co_{0.3}O_2$ was found to improve at the cost of capacity. Hence, the observed performances of the selected compound impose a limiting level of substitution as 10% for Al and 30% for Co, despite the fact that no phase in-homogeneities or structural distortions are discernible from the XRD results of the entire set of compounds chosen for the present investigation.

Generally, good capacity retention is attributed to a smaller volume change of the cathode material crystal lattice upon $Li^+$ intercalation and deintercalation process [41]. Evidently, in the present study also, the Al and Co dopants are expected to exclude any significant volume shrinkage/expansion of the interslab space of the cathode oxide lattice during the process of $Li^+$ intercalation/deintercalation. However, better cyclability and capacity retention has been realized only for $LiNi_{0.7}Co_{0.3}O_2$ and $LiNi_{0.7}Al_{0.1}Co_{0.2}O_2$ out of the five compounds studied with varying amounts of Co and Al. Probably, the excellent cyclability of Co, the inherent high capacity of Ni, and thermal stability of Al were found to co-exist (synergetic effect) in the $LiNi_{0.7}Al_{0.3-x}Co_xO_2$ solid solutions with 20 and 30% of cobalt. Therefore, it may be understood at this point that a dopant level of 20% Co and 10% Al or 30% of Co as a single dopant is essential to overcome the inherent disadvantages of $LiNiO_2$ especially with respect to capacity retention and cyclability.

The hindered $Li^+$ diffusion in $LiNi_{0.7}Al_{0.3}O_2$ indirectly affects the electrochemical performance of the compound, i.e. the hindered $Li^+$ diffusion is expected to increase the cell polarization, ultimately lowering the cycling capacity of this compound. This is obvious from the fact that $LiNi_{0.7}Al_{0\cdot3}O_2$ exhibited a decline in capacity of over 10% in 15 cycles. Furthermore, slow $Li^+$ diffusion results in small current drain, leading to an inferior rate capability. Similarly, lesser compositions of Al such as 15 and 20% were also found to suffer from capacity fade. Therefore, it may be concluded at this point that the optimum amount of Al required for the structural stability of $LiNi_{0.7}Al_{0.3-x}Co_xO_2$ compounds as 10% only, as verified from CV studies also, where the absence of phase transition has been observed only for $LiNi_{0.7}Al_{0.1}Co_{0.2}O_2$ compound.

$I_{(0\,0\,3)}/I_{(1\,0\,4)}$ ratio value of $LiNi_{0.7}Co_{0.3}O_2$ and $LiNi_{0.7}Al_{0.1}Co_{0.2}O_2$ derived from XRD, was found to be ca. 1.3, which is in further support of the better electrochemical performance of these two samples only. As a result, a trade-off between capacity and cyclability may be arrived at when Al and/or Co are substituted for Ni in the layered $LiNiO_2$ structure. However, all the five cathode oxide materials are being studied for long-term cycling and the results will be reported elsewhere.

## 5. Conclusion

A set of phase-pure Co-substituted solid solutions of the formula viz., $LiNi_{0.7}Al_{0.3-x}Co_xO_2$ ($x = 0.0$, 0.1, 0.15, 0.2, and 0.3) has been synthesized by an easy-to-adopt UAC method. Well-crystallized particles with stabilized 2D-layered structure have been obtained from UAC method. It is inferred from CV studies that the compounds are highly reversible with respect to $Li^+$ and the Co dopant is found to be effective in suppressing the phase transitions upon cycling. Among the set of five compounds synthesized, two compounds viz., $LiNi_{0.7}Co_{0.3}O_2$ (135 mAh/g) and $LiNi_{0.7}Al_{0.1}Co_{0.2}O_2$ (145 mAh/g)

are preferred for their ability to exhibit a constant deliverable capacity throughout the 15 cycles. The excellent electrochemical performance of the $LiNi_{0.7}Al_{0.1}Co_{0.2}O_2$ has been attributed to the ''synergetic effect'', an effect due to the presence of both Al and Co dopants. For better understanding of the cationic environment and the distribution in the doped compounds, investigation through ESR has been planned, as an extension of the present work. Similarly, studies concerned with the higher voltage characteristics of these types of doped compounds would be of profound relevance to the present study.

## Acknowledgements

We thank Dr. A. Mani and Dr. S. Ramu for recording PXRD and SEM, respectively. Sincere thanks are due to Dr. James Joseph for extending CV facilities. One of the authors (P.K.) is thankful to CSIR, New Delhi, for Senior Research Fellowship.

## References

[1] T. Ohzuku, M. Kitagawa, T. Hirai, J. Electrochem. Soc. 137 (1990) 769.
[2] K. Mizushima, P.C. Jones, P.J. Wiseman, J.B. Goodenough, Mater. Res. Bull. 15 (1980) 783.
[3] D. Linden (Ed.), Hand Book of Batteries, 2nd ed., McGraw-Hill Inc., NY, 1994, pp. 36.46–36.54.
[4] S. Yamada, M. Fujiwara, M. Kanda, J. Power Sources 54 (1981) 209.
[5] T. Ohzuku, H. Komori, K. Sawai, T. Hirai, Chem. Expr. 5 (1990) 733.
[6] J.R. Dahn, E.W. Fuller, M. Obrovac, U. von Sacken, Solid State Ionics 69 (1994) 265.
[7] M. Broussley, F. Perton, J. Labat, J. Power Sources 43/44 (1994) 209.
[8] Z. Zhang, D. Fouchard, J. Power Sources 7 (1998) 16.
[9] Y. Gao, M.V. Yakovleva, W.B. Ebner, Electrochem. Solid State Lett. 1 (1998) 117.
[10] H. Arai, S. Okada, Y. Sakurai, J. Yamaki, J. Electrochem. Soc. 144 (1997) 3117.
[11] Z. Liu, A. Yu, J.Y. Lee, J. Power Sources 81/82 (1999) 416.
[12] C. Delmas, I. Saadoune, A. Rougier, J. Power Sources 43/44 (1993) 595.
[13] T. Ohzuku, A. Ueda, M. Kouguchi, J. Electrochem. Soc. 142 (1995) 4033.
[14] Y.I. Jang, B. Huang, H. Wang, G.R. Maskaly, G. Ceder, D.R. Sadoway, Y.M. Chiang, H. Liu, H. Tamura, J. Power Sources 81/82 (1999) 589.
[15] R. Stoyanova, E. Zhecheva, E. Kuzmenova, R. Alcántara, P. Lavela, J.L. Tirado, Solid State Ionics 28 (2000) 1.
[16] R. Alcántara, P. Lavela, R.L. Relano, J.L. Tirado, E. Zhecheva, R. Stoyanova, Inorg. Chem. 37 (1998) 264.
[17] T. Ohzuku, T. Yanagawa, M. Kouguchi, A. Ueda, J. Power Sources 68 (1997) 131.
[18] M.K. Aydinol, A.F. Kohan, G. Ceder, J. Power Sources 68 (1997) 664.
[19] G. Ceder, Y.M. Chiang, D.R. Sadoway, M.K. Aydinol, Y.I. Jang, B. Huang, Nature 392 (1998) 694.
[20] S. Madhavi, G.V. Subba Rao, B.V.R. Chowdari, S.F.Y. Li, J. Power Sources 93 (2001) 156.
[21] D.A. Fumo, M.R. Moselli, A.M. Segades, Mater. Res. Bull. 31 (1996) 1243.
[22] W. Wang, G. Zhang, J. Xie, L. Yang, Q. Liu, J. Power Sources 82/82 (1999) 412.
[23] K.M. Lee, J. Mater. Sci. Lett. 20 (2001) 1309.
[24] C. Julien, M.A. Camacho-Lopez, T. Mohan, S. Chitra, P. Kalyani, S. Gopukumar, Solid State Ionics 135 (2000) 241.
[25] P. Kalyani, N. Kalaiselvi, N. Muniyandi, J. Electrochem. Soc. 150 (2003) A59.
[26] S.R. Jain, K.C. Adiga, V. Pai Verneker Combust. Flame 40 (1981) 71.
[27] S.S. Manoharan, K.S. Patil, J. Am. Ceram. Soc. 15 (1992) 1012.
[28] Annual Book of ASTM Standards, vol. 2, no. 5, ASTM, Philadelphia, USA, 1989, p. B527.
[29] G.T.K. Fey, J.G. Chen, V. Subramanian, T. Osaka, J. Power Sources 112 (2002) 384.
[30] J. Morales, C. Pérez-Vicente, J.L. Tirado, Mater. Res. Bull. 25 (1990) 623.
[31] T. Ohzuku, K. Nakura, T. Aoki, Electrochim. Acta 45 (1999) 151.

[32] R.K.B. Gover, R. Kanno, B.J. Mitchell, A. Hirano, Y. Kawamoto, J. Power Sources 97/98 (12001) 316.
[33] Y.I. Jang, B. Huang, H. Wang, D.R. Sadoway, G. Ceder, Y.M. Chiang, H. Liu, H. Timura, J. Electrochem. Soc. 146 (1999) 862.
[34] J. Himmrich, H.D. Lutz, Solid State Commun. 79 (1991) 447.
[35] P. Tarte, A. Rulmont, M. Leigeois-Duyclaerts, R. Cahay, J.M. Winand, Solid State Ionics 42 (1990) 177.
[36] A. Nazri, G.A. Rougier, C. Julien, Ionics 3 (1997) 170.
[37] J. Preudhomme, P. Tarte, Spectrochim. Acta 26A (1970) 747.
[38] P. Barboux, J.M. Tarascon, F.K. Shokoohi, J. Solid State Chem. 94 (1991) 185.
[39] W. Li, J.C. Curie, J. Electrochem. Soc. 144 (1997) 2273.
[40] C. Delmas, I. Saadoune, Solid State Ionics 53/54 (1992) 370.
[41] Y.K. Sun, S.H. Jin, J. Mater. Chem. 8 (1998) 2399.